Gastro Hep Advances

Regulatory T Cells play a role in determining the tumourigenicity of the Intestinal Stem Cell Niche

--Manuscript Draft--

Manuscript Number:	GHADVANCES-D-24-0059R2
Full Title:	Regulatory T Cells play a role in determining the tumourigenicity of the Intestinal Stem Cell Niche
Article Type:	Research Letter
Corresponding Author:	Lee Parry, Ph.D Cardiff University Cardiff, Wales UNITED KINGDOM
Corresponding Author Secondary Information:	
Corresponding Author's Institution:	Cardiff University
Corresponding Author's Secondary Institution:	
First Author:	Ana Padilha
First Author Secondary Information:	
Order of Authors:	Ana Padilha
	Emma Jones
	Scott Cutting
	Andrew Godkin
	Awen Gallimore
	Lee Parry, Ph.D
Order of Authors Secondary Information:	
Abstract:	Abstract no required for research letter
Order of Authors:	Ana Padilha
	Emma Jones
	Scott Cutting
	Andrew Godkin
	Awen Gallimore
	Lee Parry, Ph.D

Regulatory T Cells play a role in determining the tumourigenicity of the Intestinal Stem Cell Niche

Ana Padilha[1], Emma Jones[2], Scott Cutting, Andrew Godkin[2], Awen Gallimore[2]*, Lee Parry[1]*

[1]European Cancer Stem Cell Research Institute, School of Biosciences, Cardiff University, Cardiff CF24 4HQ, UK

[2] Systems Immunity University Research Institute / Division of Infection and Immunity, Henry Wellcome Building, School of Medicine, Cardiff, UK

**Corresponding authors*

Contact details corresponding authors:

LP – parryl3@cardiff.ac.uk, Tel. +44 (0)29 2068 8017

AG - gallimoream@cardiff.ac.uk; Tel. +44 (0) 29 2068 7012

Funding: The work was supported by an Institutional Strategic Support Fund (provided by the Wellcome Trust and National Institute for Social Care and Health Research Wales) and a Cancer Research UK PhD Studentship for AP.

Reporting and availability of data and materials: The datasets generated during and/or analysed during the current study are all fully disclosed within manuscript. Animal usage was approved by a UK Home Office Project license (PBEB09FBB; protocol 3) and data reported in accordance with UK ARRIVE guidelines (arriveguidelines.org). Requests for data and materials will be taken with consideration of relevant intellectual property.

Competing interests: The authors have no relevant financial or non-financial interests to disclose.

Abbreviations: ACF - aberrant crypt foci; CRC - colorectal cancer; IEL – intra epithelial layer; ISC - Intestinal stem cell; LI – large intestine; LPL – lamina propria layer; MLN – mesenteric lymph nodes; SI – small intestine; Treg - Foxp3^{+} regulatory T cell.

Intestinal stem cells (ISCs) are key players in maintaining the function of epithelium and barrier protection. It is now apparent that endogenous and exogenous influences impact on ISC number, plasticity, and behavior to maintain intestinal and mucosal homeostasis. Immune cells play a crucial role in this process by shaping how the ISC niche responds to such infleunces[1]. As adaptive $CD4^+$ T cells producing the cytokines IFNγ or IL-13 restrain ISC proliferation whilst driving differentiation[2]. Conversely, IL-10-producing $Foxp3^+$ regulatory T cells (Treg) maintain ISC renewal in the stem cell niche by controlling $CD4^+$T cell activation[2]. A better understanding of this immune:ISC/epithelia crosstalk is crucial to developing translational approaches to disease and healthy aging. As anti-inflammatory Treg cells maintain the *Lgr5*+ ISCs, the cell of origin for many colorectal cancers (CRC)[3]. Tregs may limit CRC risk by maintaining ISC homeostasis or controlling inflammation or, conversely, promote disease progression by inhibiting anti-tumour specific T cells (reviewed in[4]). A greater understanding on the impact of immune perturbations to the ISC population may shed light on gut health and how CRC risk may be altered. To better understand this relationship, we combined mouse models to examine the impact of Treg on ISC numbers, tumour initiation and the T cell response.

To explore at which stage Tregs begin to exert their influence we used the $Apc^{+/min}$ mouse model where, akin to CRC, tumourigenesis is driven by spontaneous *Apc* loss driving progression from aberrant crypt foci (ACF) to adenomas. At 60 days, we observed a significant increase in the density of Tregs within microadenomas ($Apc^{+/min}$T) compared to surrounding normal tissue ($Apc^{+/min}$N)(Figure 1*A* & Supplementary Figure 1*A&B*), supporting what has previously been demonstrated in $Apc^{+/min}$ adenomas[5]. Next to examine the tumour initiation phase, we used the conditional $Lgr5CreER^{T2}Apc^{flx/flx}$ model to examine Treg cells alongside conditional ISC *Apc* deletion ($Apc^{\Delta ISC}$)(Supplementary Figure 1*C*). Fifteen days following $Apc^{\Delta ISC}$ a significant increase in Tregs was observed around ACF in small and large intestine (SI & LI) compared to control mice (Figure 1*A-C* & Supplementary Figure 2*A*)

and overall *FoxP3* expression (Figure 1*D*). A significant increase in the proportion and number of Treg cells was observed in the SI intra-epithelial (IEL) and lamina propria (LPL) layers, LI IEL, spleen, and mesenteric lymph nodes (MLNs) indicating local and systemic Treg expansion following $Apc^{\Delta ISC}$ loss (Figure 1*E-G* & Supplementary Figure 3*A-C*). This data raised the possibility that Tregs are actively involved during the tumour establishment period.

To test this the $Lgr5creER^{T2}Apc^{flx/flx}$ mice were crossed with $FoxP3^{DTR}$ [6] mice to examine Treg cell depletion, following diphtheria toxin injection ($Treg^{DEP}$), alongside $Apc^{\Delta ISC}$ (Supplementary Figure 1*C*). At day 15, $Apc^{\Delta ISC}Treg^{DEP}$ mice had on average fewer ACF in the intestine that was significant in the large intestine (Figure 2*A*), supporting a role for Tregs in promoting ISC tumourgenicity. A more detailed immune cell analysis demonstrated that $Treg^{DEP}$ resulted in a significant increase in $CD4^+$ and $CD8^+$ T cells, however, this was not augmented in $Apc^{\Delta ISC}Treg^{DEP}$ mice (Figure 2*B-C*). Further in-depth immune analysis indicated that the significant elevation of $CD4^+$granzymeB$^+$, $CD4^+IFN\gamma^+$ and $CD8^+IFN\gamma^+$ observed in $Treg^{DEP}$ mice was significantly reduced in the $Apc^{\Delta ISC}Treg^{DEP}$ setting (Supplementary Figure 4A-C, other non-significant data not shown). To determine whether Treg depletion unleashes an anti-tumour immune response to $Apc^{\Delta ISC}$, through induction of IFNγ-producing, Granzyme B+ T cells capable of killing ISCs[7, 8] we administered CD4 or CD8 depleting antibodies. Surprisingly, quantification of ACF established that both $CD4^+$ and $CD8^+$ depletion significantly reduced ACF number in $Apc^{\Delta ISC}$ mice and failed to rescue this phenotype in the $Apc^{\Delta ISC}Treg^{DEP}$ mice (Figure 2*D*). This decrease in ACF due to CD4+ cell neutralisation is in keeping with an ISC homeostasis role for the CD4+ Treg cells[2]. While the impact of CD8 neutralisation may reflect the loss of CD8+αEβ7+ T-cells, as αEβ7 allows them to bind E-cadherin (to remain within the intestinal epithelium), down regulate Wnt activity and direct ISC fate via integrin signalling[9]. Thus, it appears that $CD8^+$ and possibly $Foxp3^-CD4^+$ T cells may also promote ISC tumourigenicity. The data does

however, indicate that any pro-tumorigenic effect of Tregs following *Apc* deletion in the ISC is unlikely to be due to their role in suppressing anti-tumour $CD4^+$ or $CD8^+$ T-cells.

We next considered that the impact of $Treg^{DEP}$ on the emergence of ACF may reflect their role in maintaining the normal ISC pool, as Treg depletion began 3 days prior to $Apc^{\Delta ISC}$ (Supplementary Figure 1*C*). Expression analysis in mice at day 5 indicated a significant decrease in expression of the ISC genes *Lgr5 and Ascl2* in the $Apc^{\Delta ISC}Treg^{DEP}$ mice and number compared to controls (Figure *2E-G* & Supplementary Figure 2*B*). To confirm a reduction in functional ISC numbers we performed *ex vivo* organoid culture using crypts from $Apc^{\Delta ISC}Treg^{DEP}$ mice utilising R-spondin (Rspo1; essential for $Apc^{+/+}$ organoids) to distinguish between WT and mutant ISCs. Quantification demonstrated a significant reduction in total (+Rspo1 – $Apc^{+/+}$ & $Apc^{\Delta ISC}$) and $Apc^{\Delta ISC}$ (-Rspo1) organoids because of Treg depletion (Figure 2H). This ISC reduction due to Treg loss is in keeping with previously published data[2]. With our new data demonstrating that Treg support of ISCs increases the number of cells capable of initiating a tumour following an *Apc* mutation. Evidence that CD8+ and $Foxp3^-$CD4+ T cells also influence tumorigenesis suggests that the pro-tumourigenic effects of Tregs may extend to their indirect effects on the behaviour of these T cells.

Collectively these data highlight a previously unappreciated association between Treg and altered CRC risk. Intestinal cellular homeostasis is maintained by the ISCs, which can either expand in presence of Tregs or diminish in their absence. This cross-talk may facilitate a rapid response to inflammation or injury to ensure epithelial integrity. These findings demonstrate that the role of Tregs in maintaining tissue homeostasis and responding to environmental changes is a major influence on the risk of cancer development. New therapeutic approaches that aim to reduce Treg cells to promote anti-tumour immune CRC responses[10] should also consider the impact on the CRC stem cells and normal ISC population.

Figure 1. Tregs accumulate around intestinal tumours within 15 days of *Apc* ISC loss. *(A)* Density of Treg cells in area surrounding intestinal tumour tissue (as identified by nuclear β-catenin staining; N>4 animals). *(B)* small & *(C)* large intestine IHC image showing Treg cells (Green - CD3+FoxP3+) surrounding unrecombined WT crypts or Wnt driven $Apc^{\Delta ISC}$ ACF (purple – nuclear β-catenin+) 15 days following *Apc* deletion (scale bar 20μm). *(D)* Increased relative gene expression of *FoxP3* in SI. *(E-G)* Flow cytometry quantification demonstrating compartment specific $Apc^{\Delta ISC}$ changes of CD4+ and CD4+Foxp3+ populations (Mann-Whitney U test; *P* *<0.05, **<0.01, ***<0.001 or ****<0.0001).

Figure 2. Reduction in intestinal tumourigenesis due to Treg depletion is due to altered immune:ISC crosstalk rather than immune elimination. *(A)* Quantification of ACF 15 days following ISC *Apc* loss and/or Treg depletion. *(B&C)* Cell quantification demonstrating $Apc^{\Delta ISC}Treg^{DEP}$ specific immune changes in LI IEL (left) & LI LPL (right). *(D)* Quantification of ACF following neutralization of CD4+ or CD8+ cells. *(E&G)* Downregulation of ISC markers in *Lgr5* & *Ascl2* due to Treg depletion. *(H)* Quantification of organoids derived *ex vivo* from $Apc^{\Delta ISC}Treg^{DEP}$ intestinal crypts at day 5 indicating loss of functional ISCs. (Mann-Whitney U test; *P*: 1-tailed ☆<0.05; 2-tailed *<0.05, **<0.01, ***<0.001 or ****<0.0001).

References

1. Choi J, Augenlicht LH. Intestinal stem cells: guardians of homeostasis in health and aging amid environmental challenges. Exp Mol Med 2024;56:495-500.
2. Biton M, Haber AL, Rogel N, et al. T Helper Cell Cytokines Modulate Intestinal Stem Cell Renewal and Differentiation. Cell 2018;175:1307-1320 e22.
3. Barker N, Ridgway RA, van Es JH, et al. Crypt stem cells as the cells-of-origin of intestinal cancer. Nature 2009;457:608-11.
4. Olguín JE, Medina-Andrade I, Rodríguez T, et al. Relevance of Regulatory T Cells during Colorectal Cancer Development. Cancers (Basel) 2020;12.
5. Akeus P, Langenes V, von Mentzer A, et al. Altered chemokine production and accumulation of regulatory T cells in intestinal adenomas of APC(Min/+) mice. Cancer Immunol Immunother 2014;63:807-19.
6. Kim JM, Rasmussen JP, Rudensky AY. Regulatory T cells prevent catastrophic autoimmunity throughout the lifespan of mice. Nat Immunol 2007;8:191-7.
7. Takashima S, Martin ML, Jansen SA, et al. T cell-derived interferon-gamma programs stem cell death in immune-mediated intestinal damage. Sci Immunol 2019;4.
8. Hoek KL, Greer MJ, McClanahan KG, et al. Granzyme B prevents aberrant IL-17 production and intestinal pathogenicity in CD4(+) T cells. Mucosal Immunol 2021;14:1088-1099.
9. Chen S, Zheng Y, Ran X, et al. Integrin alphaEbeta7(+) T cells direct intestinal stem cell fate decisions via adhesion signaling. Cell Res 2021;31:1291-1307.
10. Scurr M, Pembroke T, Bloom A, et al. Effect of Modified Vaccinia Ankara-5T4 and Low-Dose Cyclophosphamide on Antitumor Immunity in Metastatic Colorectal Cancer: A Randomized Clinical Trial. JAMA Oncol 2017;3:e172579.

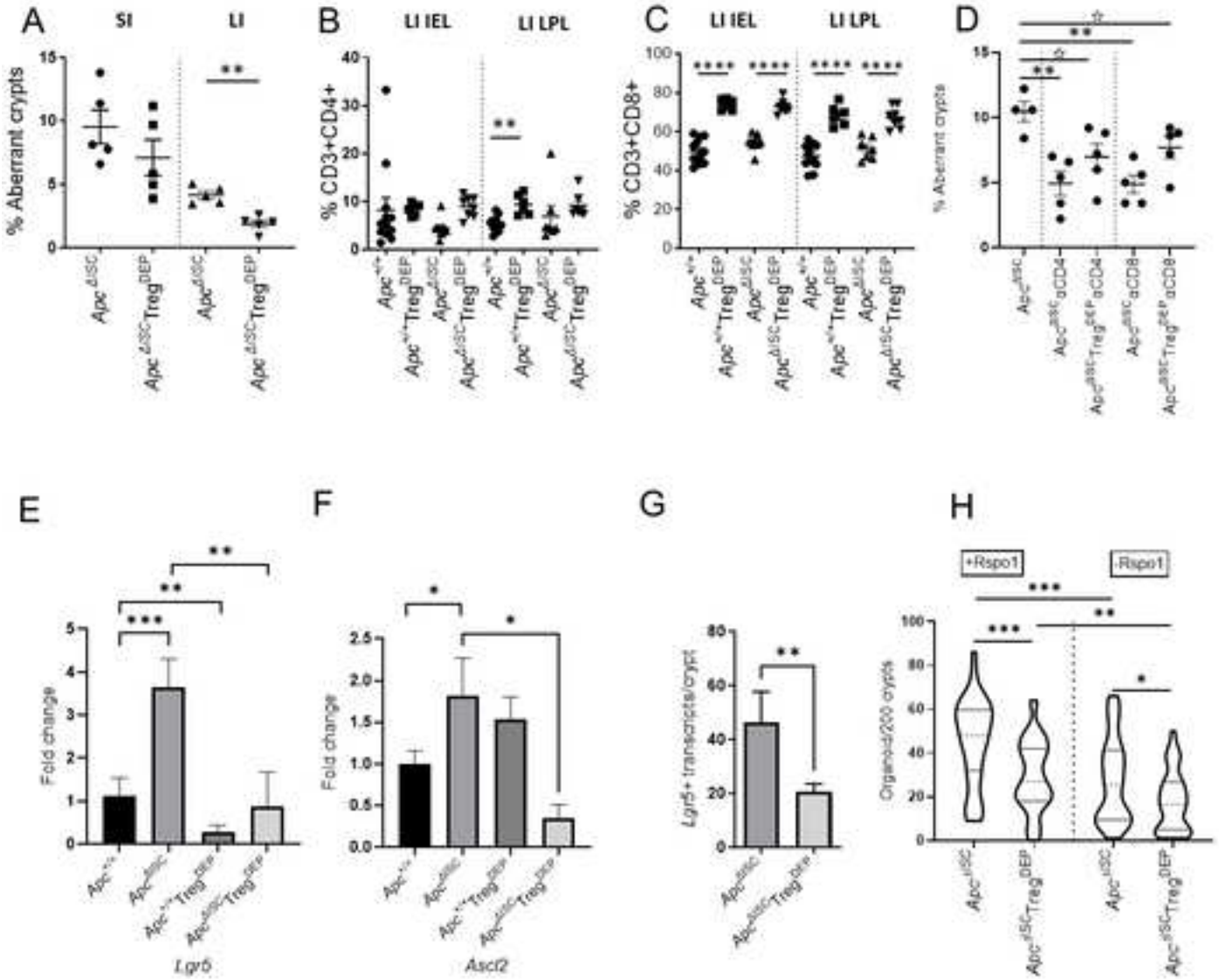

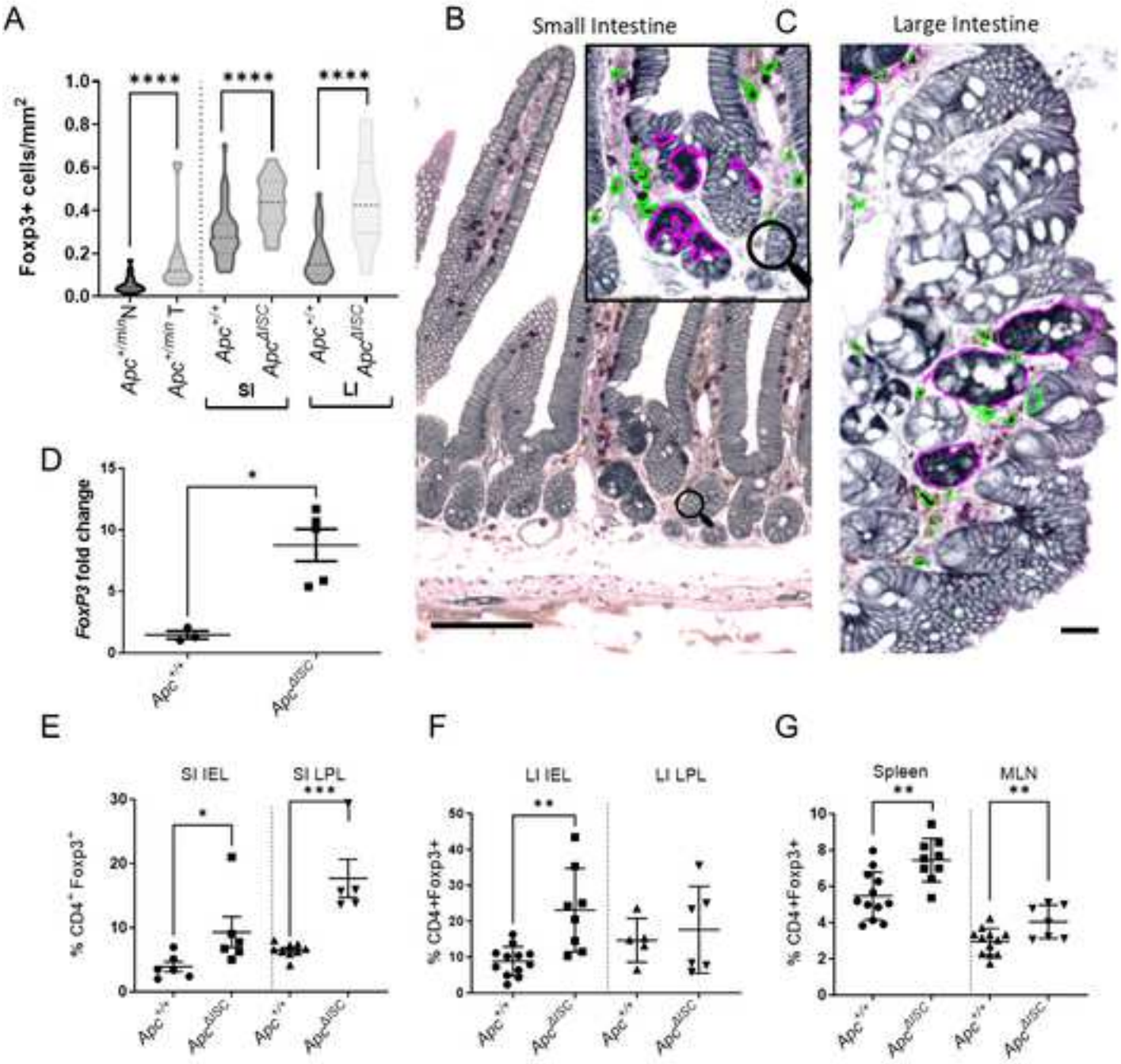

Clean accepeted manuscript

Click here to view linked References

SUPPLEMENTAL INFORMATION

Regulatory T Cells play a role in determining the tumourigenicity of the Intestinal Stem Cell Niche

Ana Padilha[1], Emma Jones[2], Scott Cutting, Andrew Godkin[2], Awen Gallimore[2]*, Lee Parry[1]*

Animal Models

Lgr5Cre^{ERT2} *Apc*$^{fl/fl}$ *Foxp3*^{DTR} mice were bred in a specific pathogen-free (SPF) barrier facility and housed in conventional facilities during procedures. Equivalent numbers of male and female mice between 10 and 15 weeks old were entered at the start of experiments.

Induction of the *Lgr5Cre*^{ERT2} transgene was achieved by administering a single intraperitoneal injection (IP) of 10mg/ml tamoxifen (TAM; 80 mg/kg; Sigma-Aldrich) mixed in corn oil (Sigma-Aldrich) for four consecutive days. For *in vivo* depletion of Foxp3+ Treg cells 15 µg/Kg diphtheria toxin (DT; Sigma-Aldrich), diluted in sterile phosphate buffered saline (PBS; ThermoFisher Scientific) was IP injected every other day for 15 days, starting a day prior to TAM injection. Depleting CD4-specific antibodies were produced in house (1). Mice were injected with 2 mg of anti-CD4 antibodies (clones YTS-191 and YTA-3) prior to TAM and again one week later. CD8+ cell depletion was achieved by IP injection of 250ug of the depleting anti-CD8 monoclonal antibody (clone YTS-169) (Bioxcell), a day prior to TAM injection and 100 µg one week later. All experiments were repeated at least twice.

Intestinal Epithelial Cells Extraction for Gene Expression Analysis

Following dissection, a section of the small intestine (between the 5th and 12th cm) was opened longitudinally and cut into small fragments. Fragments were washed gently with HBSS containing HEPES (1:100) before the supernatant was discarded and 10 ml 8 mM EDTA (Sigma-Aldrich) was added for incubation on ice for 30 min. Following incubation, tubes containing the fragments were shaken vigorously and the supernatant collected into a fresh 50ml tube containing 10 ml complete RPMI 1649 medium supplemented with GlutaMAX (Life Technologies), penicillin/streptomycin (Thermo Fisher Scientific) and 10% Foetal Bovine Serum (FBS) (Thermo Fisher Scientific). This process was repeated before fragments were filtered through a 70 µm cell strainer (MACS) and supernatant collected and spun down at 1000 rpm for 5 minutes. The resulting pellets were re-suspended in 1ml RNA later (Sigma-Aldrich). RT-qPCR was performed as previously described (2). Oligonucleotide sequences and probes used for relative quantification are available upon request.

Immunohistochemistry (IHC) and cellular analysis

Small and large intestines were collected, opened longitudinally, rolled and fixed in ice-cold 10% formalin (Sigma-Aldrich) for 24 hours before processing into wax blocks. Sections were cut at 5 µm thickness and rehydrated. Staining was performed using the anti-rat (mouse adsorbed), anti-mouse, and anti-rabbit ImmPRESS HPR kits (Vector Labs) according to the manufacturer's instructions. The following antibodies were used for immunohistochemistry: anti-β-catenin (BD Biosciences), anti-Foxp3 (eBioscience), anti-CD4 (eBioscience), anti-CD8 (eBioscience) and anti-CD3 (DAKO). Samples were incubated with secondary antibody and

signal visualized with an enzyme-specific, chromogenic colour, according to manufacturer's recommendations. Tissue was counterstained in hematoxylin, dehydrated and mounted in distyrene, plasticizer, xylene mountant (DPX; Sigma-Aldrich). To quantify histological sections the images that were acquired in the Zeiss Axio Scan.Z1 slide scanner were analysed using the ZEN image analysis software. At least four mice per cohort were analysed. To analyse the total tumour burden, the whole crypts touching the basement membrane with positive nuclear B-catenin staining (aberrant crypts), from both small and large intestines, were counted. The paraffin embedded tissues were cut into three serial sections separated by 120 µm distance to avoid the quantification of the same aberrant crypts. A total of five mice were analysed. Data was normalised by counting the total number of whole crypts touching the intestinal basement membrane. Partial tumour burden was analysed by assessing the number of whole crypts with positive nuclear B-catenin in 100 crypts of the first 5 cm of the small intestine. The average number of aberrant crypts was calculated and the mean across the cohorts was determined. A minimum of four mice were analysed.

The number of Treg was determined by co-B-catenin-CD3-Foxp3 IHC staining. For *Apc*$^{+/min}$ tumours CD3+FoxP3+Tregs were counted within the adenoma as identified by B-catenin staining. For the *Lgr5creApc*$^{flx/flx}$ mice Tregs were quantified around unrecombined *Apc*$^{flx/flx}$ or *Apc*$^{\Delta ISC}$ crypts as identified by β-catenin nuclear staining in the: (1) small intestine - the region between the crypt:villus junction and the basement membrane and (2) large intestine-region immediately surrounding the normal or aberrant crypts with a minimum number of five fields of view of at least 50µm^2. Cells were quantified from 25 normal and 25 aberrant whole crypts. A minimum of four mice were analysed. The average number of positive cells was calculated and the mean across the cohorts was determined.

Isolation of Lymphocytes and Flow Cytometry Analysis

Spleen and MLN were homogenized using the back of a 1ml syringe plunger through a 70 µm cell strainer (MACS). Red blood cells in spleen were lysed using RBC lysis buffer (Sigma) Small (SI) and large (LI) intestines were open longitudinally, cut into small fragments and placed into 50 ml tubes with HBSS containing HEPES buffer. Intra epithelial (IEL) and lamina propria (LPL) lymphocytes were obtained as previously described (3).

Cells were washed in PBS, stained using an aqua amine-reactive viability dye (LIVE/DEAD Aqua, Invitrogen), then washed. Fc receptors were blocked with anti-CD16/32 (clone 93; eBioscience) before staining with surface antibodies to CD3 (AF488, eBioscience), CD4 (BV421, BD Bioscience) and CD8 (APC-H7, BD Bioscience). For intracellular staining, cells were stimulated in 96-well plates with 50 ng/ml phorbol myristate acetate (PMA; Sigma – Aldrich) and incubated with 1 µl/ml ionomycin (Sigma – Aldrich) and 5 µg/ml brefeldin A (Sigma – Aldrich) for 3h. Prior to intracellular staining with with Foxp3 (PeCy7, eBioscience),

granzyme B (APC, Biolegend), IL-17A (PE, BD Pharmingen) and IFNγ (PE-Pharmingen) specific antibodies, cells were fixed/permeabilized according to the manufacturer's protocol (Foxp3-staining kit; eBiosciences). Data were acquired on a NovoCyte ® 3000 cytometer and analysed using FlowJo version 10 and NovoExpress software.

RNAscope

In situ detection of *Lgr5* mRNA transcripts using the RNAscope kit 2.5 HD Assay-BROWN (Advanced Cell Diagnostics, Hayward, CA, USA) was performed according to the manufacturer's protocol. Positive staining was determined by brown punctate dots and their quantification was performed at the crypt base in a total of 30 crypts per mouse; the average number of brown dots was calculated and the mean across the cohorts was determined.

Ex vivo analysis

Mice were harvested and 200 intestinal crypts per well were plated in Matrigel in Intesticult™ organoid culture medium (Stemcell technologies, UK). Medium was replaced every 2 days and organoid number determined at day 7 (Gelcount, Oxford Optronix, UK).

Statistical analysis

Data were analysed using Graph Pad Prism 10 software as indicated in figure legends. All relevant comparisons where significant differences exist are indicated on graphs (2-tailed Mann-Whitney * *P<.05, ** P<.01, *** P<.001 & **** P<.0001*).

Acknowledgements

Authors would like to thank Mark Bishop, Jolene Twomey and Carys Holmes for technical support during this project.

Supplementary Figure 1. IHC image of (A) normal and (B) microadenoma (black outline; β-catenin-grey) tissue from a 60-day old *Apc*$^{+/min}$ mouse showing adenoma specific accumulation of Treg cells (black arrows FoxP3+-brown; scale bars = 20). (C) Schematic indicating agents and administration regimes for conditional transgenes and neutralising antibodies.

Supplementary Figure 2. (A) IHC image of normal intestine demonstrating low residual numbers of Treg cells in the absence of *Apc* loss (Black arrows indicate Treg cells; β-catenin-grey, CD3-purple & FoxP3-brown; scale bar = 100μm). (B) RNAscope® images indicating gain of *Lgr5* transcripts upon *Apc*$^{\Delta ISC}$ opposed to their loss following Treg depletion (*Lgr5* transcripts highlighted by black arrows in left panel, scale bar = 50μm).

Supplementary Figure 3. (A) Flow cytometry plots demonstrating number of Tregs in intestine (CD4+FoxP3+ cells)(*Apc*$^{+/+}$ - left hand column & *Apc*$^{\Delta ISC}$ right hand column). (B&C) Quantification of absolute numbers by flow cytometry of CD4+FoxP3+ in intestine 15 days following ISC *Apc* loss (P value *<0.05).

Supplementary Figure 4. (A-C) Significant changes observed upon flow cytometry of large intestine IEL (left panels) and LPL (right panels) immune cells 15 days following manipulation of ISC *Apc* and Treg status (P value *<0.05 & **<0.01).

Supplementary References

1. Golgher-D. et al. EJI. 2002,
2. May S. et at. J Pathol. 2018, **245**: 270-281.
3. Uhlig H. et al. J Immunol. 2006, **177(9)**: 5852-5860.